Surface Analysis of Silica Gel Particles after Mechanical Dry Coating with Magnesium Stearate

Laurence Galet‡, Yamina Ouabbas**, Alain Chamayou*, Philippe Grosseau**, Michel Baron*, Gérard Thomas****

(Received: May 2010)

* Dr. L. Galet (‡ corresponding author), Dr. A. Chamayou, Prof. M. Baron, Ecole des Mines d'Albi-Carmaux, Centre RAPSODEE, UMR CNRS 2392, Campus Jarlard 81013 Albi Cedex 9 (France).

E-mail: laurence.galet@mines-albi.fr

** Dr. Y. Ouabbas, Dr. P. Grosseau, Prof. Dr. G. Thomas, Ecole Nationale Supérieure des Mines de Saint Etienne, Centre SPIN – LPMG -UMR CNRS 5148, 158 Cours Fauriel 42023 Saint-Etienne Cedex 2 (France).

Abstract

A dry coating technique has been used to change the surface properties of silica gel particles (d_{50} = 55 μm) by coating with different mass ratios of magnesium stearate - $MgSt_2$ (d_{50} = 4.6 μm): 1%, 5%, 15% and 30%. The dry coating experiments were performed using a "Hybridizer, a high-speed dry impact blending coater", manufactured by Nara Machinery (Japan). The surface morphology of the uncoated and coated silica gel particles was observed by environmental scanning electron microscopy (ESEM). The images show that a greater $MgSt_2$ coverage was observed on the surface of silica gel as the $MgSt_2$ mass ratio is increased. In addition, atomic force microscopy (AFM) analysis revealed how this coating process makes possible a discrete and uniform dispersion of the $MgSt_2$ particles. AFM studies were carried out with a scanning probe microscope Multimode Nanoscope IIIA (Digital Instruments/Veeco Metrology Group).

Keywords: AFM phase imaging, adhesion force, dry coating, silica, magnesium stearate.

1 Introduction

Dry particle coating to change the surface properties of powders is very important in many industries. Typical applications include, but are not limited, to flowability, wettability (hydrophobic/hydrophilic properties), solubility, dispersibility, flavour, shape, electrostatic, optical, electric, magnetic, etc. In dry particle coating processes, materials with relatively large particle size (host particles; 1-500 μm) are mechanically coated with fine particles (guest particles; 0.1-50 μm) in order to create new functionality or to improve their initial characteristics [1]. Since the size of the guest particles are so small, van der Waals interactions are strong enough to keep them firmly attached to the host particles. Thus,

either a discrete or continuous coating of guest particles can be achieved depending on a variety of operating conditions including processing time, rotation speed, weight fraction of guest to host particles and particle properties [2]. Figure 1 below is a simple schematic illustrating the process of dry particle coating.

Over the last few years, we have performed experimental investigations of applications of the dry coating technique to study the effect of mechanical dry coating on the surface properties of powders. Our recent work is related to the modification of the flowability and the wettability properties of silica gel particles coated with different weight ratios of magnesium stearate by using a high energy impact coater Hybridizer from Nara Machinery [3] and a high shear mixer Cyclomix from Hosokawa [4]. For example, the flowability of the silica gel powder was significantly decreased after treatment in the Cyclomix mixer with 15% of $MgSt_2$. Moreover, it has been found that the coating by hydrophobic $MgSt_2$ in the Cyclomix can reduce the high affinity between silica gel and water after treatment with 5% and 15% of MgSt. In those papers, it has been demonstrated that a dry particle coating technique can be used to modify the properties of silica gel powder by coating with small quantities of hydrophobic magnesium stearate in both the Hybridizer and the Cyclomix. The more uniform coating has been obtained after treatment in the Hybridizer device.

Figure 1. Schematic principle of dry coating.

In this paper, we report an investigation of the surface analysis of the coated silica gel particles using atomic force microscopy in tapping mode (TM-AFM) and contact mode (CM-AFM). The TM-AFM method, based on the measurements of the oscillations of a cantilever probe in contact on the sample, has been used for several years to characterize the surface topography of particles. In particular, phase contrast images are related to characterize the attractive and repulsive probe sample interactions [5], the sample surface

components [6] and the morphology of composite particles [7]. The CM-AFM method consists in using a colloidal probe fixed on the cantilever to quantify the adhesion force between the particles. As an example, Kani et al report an interesting study on the silica-mica adhesion force as a function on the presence of impurities on the silica particles [8]. Meincken et al. report a relationship between contact angle analysis and adhesive forces measurements by the AFM technique in a study of the surface hydrophobicity of polyurethane coatings [9]. This technique has been also used to characterize the adhesion properties of pharmaceutical carriers [10]. In our case, we performed AFM phase-contrast and adhesion forces measurements to characterize the surface of silica particles as a function of the magnesium stearate mass ratio (1 to 30%).

2 Experimental

2.1 Powders

Silica gel powder supplied by Merck and usually used for filling chromatography columns has been chosen as host particles for dry coating (Silica gel 60, 0.040-0.063 mm). The volume distribution of silica gel shows a population of large particles with median diameter (d_{50}) of about 55 μm. Hydrophobic magnesium stearate ($MgSt_2$) supplied by Chimiray is used as guest particles. The $MgSt_2$ is a fine, white, greasy and cohesive powder widely used in pharmaceutical formulation as a lubricant. A wider size distribution is observed for $MgSt_2$ particles. The size of $MgSt_2$ particles varies between 20 μm to less than 1 μm with a median diameter (d_{50}) of about 4.6 μm. The main properties of host and guest particles are reported in the Table 1.

Table1: Properties of host and guest particles.

2.2 Coating process

The hybridization system (HB, type NHS-0; Nara Machinery Co.), a high-speed dry impact blending coater, has been used to make the silica gel-$MgSt_2$ composite particles. The reactor consists in a very high-speed rotating rotor with six blades, a stator and a powder re-circulation circuit. The coating chamber is surrounded with a jacket in which coolant is circulated [1]. The coating process can be summarized as follows: the powder mixture (host and guest particles) is subjected to high impaction and dispersion due to collisions with blades and the walls of the device and continuously re-circulates in the machine through the cycle tube. Particle coating is achieved due to the embedding or filming of the guest particles onto the host particles by high impaction forces and friction heat. Since the rotor of the hybridizer can rotate from 5000 to 16000 rpm, very short processing time is required to achieve coating. The operating conditions used in experiments are 4800 rpm for 5 min. The preparation of the coated particles is described in detail in previous papers [3, 4]. Coating experiments have been carried out with 1%, 5%, 15% and 30% of mass fraction of guest $MgSt_2$ particles.

2.3 Particles characterization

The uncoated and coated silica gel particles were examined by environmental scanning electron microscopy (ESEM) to study the surface morphology and the covering by the $MgSt_2$ particles (XL 30 Philips). The ESEM images reveal that greater $MgSt_2$ coverage is observed on the surface of silica gel particles as the percentage of $MgSt_2$ is increased (Figure 2). Additional investigations were done to analyse the surface atomic composition of the coated particles by X-ray spectroscopy confirming the presence of magnesium atoms

when analysis is performed on a black spot [11]. At 15%, the surface coverage of the $MgSt_2$ is intense but seems discrete.

Figure 2. ESEM images of silica gel and $MgSt_2$-silica gel coated particles.

Thermal analysis was used to measure the $MgSt_2$ mass fraction after treatment (TG-DSC 11 Setaram). Samples are analyzed under nitrogen gas, from 20°C to 600°C, with a ramp of 5°C/min. Figures 3 and 4 show the heat flow, the mass lost and the differential mass lost as a function of the temperature diagram for pure silica gel and $MgSt_2$, respectively. We observe that the silica gel particles have a main first mass loss of about 4-5% near 100°C, due to dehydration, and a second near of 2% 400-600°C, probably due to a thermal decomposition. The $MgSt_2$ has a first small mass loss near 100°C due to dehydration and a main mass loss of 85-90% between 250°C and 450 °C due to a thermal degradation. This mass loss can be used to quantify the $MgSt_2$ in the powder mixtures.

Figure 3. TG-DSC diagrams for silica gel.

Figure 4. TG-DSC diagrams for $MgSt_2$.

TG-DSC experiments have been performed on silica gel-$MgSt_2$ mixtures made by manual mixing (1%, 3%, 15%, 30% and 50% mass ratios). The loss of mass obtained between 250°C and 600°C as a function of the $MgSt_2$ ratio is reported in the Figure 5. This result is the mean of two measurements. The results show a very good relation between the AGT-DSC mass loss (%) as a function of the $MgSt_2$ ratio (%). The linear relation obtained with a high correlation coefficient has been used to calculate the real composition of the coated particles after processing in the reactor with a precision of less than ±1%.

Figure 5: Experimental relation between the TG-DSC mass loss (from 250°C to 600°C) and the mass ratio of $MgSt_2$.

AFM measurements were made with a Multimode Nanoscope IIIA from Veeco Metrology Group. In tapping mode, the cantilever is driven to oscillate. Height, amplitude and phase images were simultaneously recorded for each sample. Beyond the standard height imaging, the phase contrast mode is quite efficient to exhibit the main surface property differences between de silica gel and $MgSt_2$.

The amplitude and the frequency of the oscillations change when the tip scans on a surface. TM-AFM images are produced by imaging the oscillating contacts of the tip with the sample surface: height and amplitude images give information on the sample surface topography and phase images give information on the atomic surface composition (interaction tip-surface). The TM-AFM measurements were performed with a MPP 11100 Silcon phosphorus doped silicium tip with a spring constant of 40 N/m. Large surface scale of surface sample has been scanned: from 250x250 nm^2 to 5x5 mm^2, for silica gel and silica gel-$MgSt_2$ coated particles (1%, 5% and 15% $MgSt_2$ mass ratio).

In contact mode AFM, the tip scans the sample in close contact with the surface. The force between the tip and the surface sample is measured as the distance, by maintaining a constant deflection. To examine the mechanism of interaction between silica gel and $MgSt_2$ particles, the CM-AFM measurements were performed with a NP silicon nitride tip with a spring constant of 0.32 N/m on which a $MgSt_2$ particle was glued under optical microscope. The adhesion forces were measured between the $MgSt_2$ particles attached on the end of the cantilever and the different samples of uncoated and coated particles with 1% to 30% $MgSt_2$ mass ratio. For each sample 450 force curves were obtained. The presence of the magnesium stearate particle on the tip was checked after each series of measurements.

Influence of the coating on the surface property of the silica gel particles was also studied. The sessile drop method was used to study the wettability of the different samples. We report the contact angle value of a water drop (10 µl) deposited on different particulate systems: pure silica gel, pure $MgSt_2$ and coated particles. The method performed is described in details in previous papers [3, 4].

3 Results and Discussion

The real concentration of the $MgSt_2$ after coating is calculated from the TG-DSC measurements and the calibration straight line shows in Figure 5. The results are reported in the Figure 6. This loss of $MgSt_2$, due to a deposit of $MgSt_2$ on the coating chamber surface, varies as a function of the introduced $MgSt_2$ mass ratio. That is from 30% for the sample containing initially 30% of $MgSt_2$ in the mixture, to 40% for the sample containing initially 5% $MgSt_2$ in the mixture.

Figure 6: Real mass fraction of $MgSt_2$ after the coating process calculates from the mass loss.

The phase imaging TM-AFM characterisations of the samples are reported in Figure 7. Concerning the $MgSt_2$, the amplitude image reveals an irregular surface topography. The phase contrast image shows various levels of phase contrast (black and white areas), which can reach 50°. The silica gel particles have a more regular surface topography, formed by spherical micro beads (about 100 to 600 nm) and a low phase contrast only due to the topography (from 0° to 10°). The analyses of the silica-$MgSt_2$ coated particles clearly reveal a modification of the surface due to the presence of the magnesium stearate, even at 1% of $MgSt_2$ introduced. With a $MgSt_2$ initial mass ratio of 15%, both the amplitude and the phase

contrast images evolve into the pure $MgSt_2$ images. For the coated particles, the part of the image characterized by high phase angles can be attributed to the presence of $MgSt_2$ layers on the surface of silica gel.

Figure 7. TM-AFM images of $MgSt_2$, silica gel and silica coated with 1% and 15 % initial mass ratios of $MgSt_2$ (2x2 μm^2).

The contact mode analyses bring some pertinent information about the silica gel covering by the magnesium stearate. Figure 8 gives an adhesion force–displacement curve for the pure products. The force measured between a particle of $MgSt_2$ fixed onto the AFM tip is about 10 nN for the pure silica gel particle. That is near 120 nN for the $MgSt_2$-$MgSt_2$, revealing a high interaction.

Figure 8: Force curves F (N/m) as a function of the distance z (μm) measured with $MgSt_2$ sticked on the tip for pure silica gel and pure $MgSt_2$.

Figure 9: CM-AFM adhesion force distribution obtained with 450 analyses for different particulate systems.

The adhesion force distributions for the different particulate systems are reported in the Figure 9. These distributions were obtained from 450 measurements of each particulate system. This force varies proportionally to the quantity of $MgSt_2$ introduced and confirms the increasing presence of the $MgSt_2$ on the silica gel surface when the mass ratio increases. For the coated particles, the number of high adhesion forces increased as the mass ratio of $MgSt_2$ increases. The mean adhesion force between the $MgSt_2$ particles attached on the end of the cantilever and the $MgSt_2$ sample (68 nN) was stronger than for the silica gel sample (8

nN). The large distribution of the adhesion forces confirm the discrete deposition of the $MgSt_2$ particles onto the surface silica gel particles as observed by the ESEM images.

The mean adhesion force calculated from the 450 measurements for each system is reported in the Table 2. The results show an increasing of the mean value of the force as a function of the increasing of the $MgSt_2$ concentration. The mean adhesion force seems to evolve progressively to the mean value of the pure $MgSt_2$ (Figure 10). This no linear evolution could be due to a random distribution of the $MgSt_2$ particles on the silica gel surface.

Table 2: Mean adhesion force (nN) for different particulate systems.

Figure 10: Mean adhesion force (nN) as a function of the sample $MgSt_2$ concentration.

The affinity of water is evaluated by the behaviour of a water drop deposited on the particulate systems. The initial contact angle values are reported in Table 3. The Figure 11 shows the evolution of the contact angle as a function of the $MgSt_2$ ratio. We observe a increasing of the contact angle of the water drop as the presence of the $MgSt_2$ on the silica gel surface. This result is of course in agreement with the hydrophobicity of this compound. However, even with a low content of $MgSt_2$, the contact angle measured is significatively modified: 70° and 110° for 0.1% and 1.1% $MgSt_2$ respectively. The surface property of the silica gel particles is modified by dry coating even with a very low ratio of $MgSt_2$. This result reveal that at the water drop scale, a very few presence of $MgSt_2$ is enough to modify the hydrophilic property of the silica gel.

Table 3: Contact angle measurements (°) for different particulate systems.

Figure 11: Contact angle measurements (°) as a function of the sample $MgSt_2$ concentration.

4 Conclusion

Dry particle coating can be used to create new generation materials with altered properties or new functionalities. This treatment creates a discrete or a continuous coating of fine particles on the surface of the large particle surface. In this study a Nara Hybridizer has been used as a dry coating device for the coating of silica gel particles with different mass ratios of $MgSt_2$ particles. ESEM observations show that $MgSt_2$ particles form a discrete coating onto the surface silica gel particles. The $MgSt_2$ surface coverage increases and the surface becomes more and more uniform as the mass ratio of $MgSt_2$ is increased. In addition to ESEM observations, AFM images and distributions curves of adhesion forces confirm the distribution of $MgSt_2$ in discrete layers onto the silica gel surface. The mean adhesion force obtained for the different particulate systems reveal a no linear evolution to the adhesion force measured for the pure $MgSt_2$. From these results, we are currently working on the development of a distribution model of $MgSt_2$ particles onto the surface of silica gel based on the adhesion force results. The sessile drop method reveals that a discrete deposition of the $MgSt_2$ allows a real modification of the hydrophilicity of the silica gel. Less than 3% of $MgSt_2$ is enough to increase the contact angle near the value of the pure $MgSt_2$. This additional approach confirms the efficiency of the dry coating technique to design some new composite systems with controlled end use properties.

5 Acknowledgements

The authors would like to acknowledge Sylvie Delconfetto for the TG-DSC measurements and Christine Rolland for the ESEM images.

6 Nomenclature

AFM	Atomic Force Microscopy
CM-AFM	Contact Mode Atomic Force Microscopy
ESEM	Environmental Scanning Electron Microscopy
$MgSt_2$	Magnesium Stearate
TM-AFM	Tapping Mode Atomic Force Microscopy

7 References

[1] I. Yoshihara, W. Pieper, Hybridization – Technology for surface modification of powders without binders, *Swiss Pharma*. **1999**, *21*, 6.

[2] R. Pfeffer, R.N. Dave, W. Dongguang, M. Ramlakhan, Synthesis of engineered particulates with tailored properties using dry particle coating, *Powder Technology* **2001**, *117*, pp.40-67.

[3] Y. Ouabbas, A. Chamayou, L. Galet., M. Baron, G. Thomas, P. Grosseau, B. Guilhot, Surface modification of silica particles by dry-coating: Characterization and powder ageing, *Powder Technology* **2008**, in press.

[4] Y. Ouabbas, J.A. Dodds, L. Galet., A. Chamayou, M. Baron, Particle-particle coating in a cyclomix impact mixer, *Powder Technology* **2008**, in press.

[5] X. Chen, C.J. Roberts, J. Zhang, M.C. Davies, S.J.B. Tendler, Phase contrast and attraction-repulsion transition in tapping mode atomic force microscopy, *Surface Science* **2002**, *519*, pp. L593-598.

[6] A. Danesh, X. Chen, M.C. Davies, C.J. Roberts, G.H.W. Sanders, S.J.B. Tendler, P.M. Williams, M.J. Wilkins, *Langmuir* **2002**, *16*, pp. 866-870.

[7] V.M. Gun'Ko et al, Composite powders with titania grafted onto modified fumed silica, *Powder Technology* **2006**, *164*, pp. 153-167.

[8] T. Kani, M. Tamonoki, T. Suzuki, M. Tsukada, H. Kamiya, Influence on the surface-adhered nanoparticles and nanoporous structure on particle-particle interaction of silica, *Powder Technology* **2007**, *176*, pp. 99-107.

[9] M. Meincken, A. Klash, S. Saboa, R.D. Sanderson, Influence of the viscosity and the substrate on the surface hydrophobicity of polyurethane coatings, *Applied Surface Science* **2006**, *253*, pp. 805-809.

[10] M. Louey, P. Mulvaney, P.J. Stewart, Characterization of adhesional properties of lactose carriers using atomic force microscopy, *Journal of Pharmaceutical and Biomedical analysis* **2001**, *25*, pp. 559-567.

[11] Y. Ouabbas, *Procédés mécaniques d'élaboration à sec de particules composites à propriétés d'usage contrôlées – Caractérisation et stabilité d'un gel de silice*, PhD Thesis, Ecole Nationale Supérieure des Mines de Saint-Etienne, N°467GP, **2008**.

Legends of Tables

Table1: Properties of host and guest particles.

Table 2: Mean adhesion force (nN) for different particulate systems.

Table 3: Contact angle measurements (°) for different particulate systems.

Legends of figures

Fig. 1: Schematic principle of dry coating.

Fig. 2: ESEM images of silica gel and $MgSt_2$-silica gel coated particles.

Fig. 3: TG-DSC diagrams for silica gel.

Fig. 4: TG-DSC diagrams for $MgSt_2$.

Fig. 5: Experimental relation between the TG-DSC mass loss (from 250°C to 600°C) and the mass ratio of $MgSt_2$.

Fig. 6: Real mass fraction of $MgSt_2$ after the coating process calculates from the mass loss.

Fig. 7: TM-AFM images of $MgSt_2$, silica gel and silica coated with 1% and 15 % initial mass ratios of $MgSt_2$ (2x2 μm^2).

Fig. 8: Force curves F (N/m) as a function of the distance z (μm) measured with $MgSt_2$ sticked on the tip for pure silica gel and pure $MgSt_2$.

Fig. 9: CM-AFM adhesion force distribution obtained with 450 analyses for different particulate systems.

Fig. 10: Mean adhesion force (nN) as a function of the sample $MgSt_2$ concentration.

Figure 11: Contact angle measurements (°) as a function of the sample $MgSt_2$ concentration.

Table1: Properties of host and guest particles.

Particles	Size (d_{50}) (μm) (Mastersizer 2000)	Solid density (g/cm^3) (Helium Pycnometer)	Specific surface area (SBET (m^2/g)	Pore Volume (cm^3/ g)
Silica gel	55 (D_{host})	2.07 (ρ_{host})	475	0.69
MgSt	5 (d_{guest})	1.04 (ρ_{guest})	7.7	0.02

Table 2: Mean adhesion force (nN) for different particulate systems.

Sample	Mean adhesion force (nN)
Pure silica gel	8
Silica gel + 2.95 % MgSt	13
Silica gel + 9.93 % MgSt	23
Silica gel + 21.51 % MgSt	35
Pure MgSt	68

Table 3: Contact angle measurements (°) for different particulate systems.

Sample	Contact angle (°)
Pure silica gel	15±3
0.1 %	70±7
1.1 %	110±5
3.0 %	112±5
9.9 %	116±3
Pure MgSt	125±6

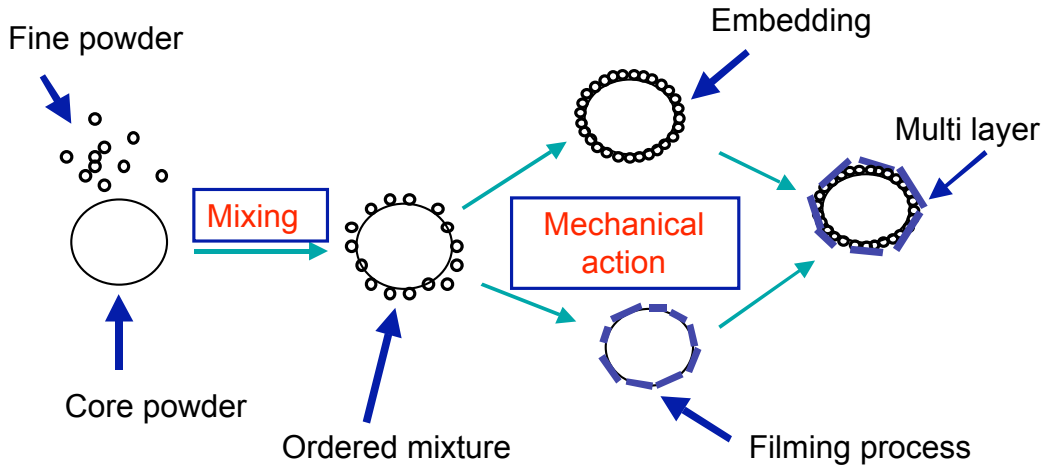

Fig. 1: Schematic principle of dry coating.

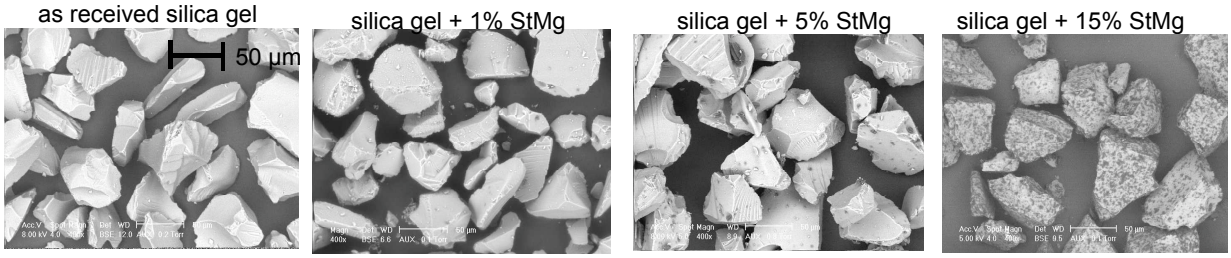

Fig. 2: ESEM images of silica gel and $MgSt_2$-silica gel coated particles.

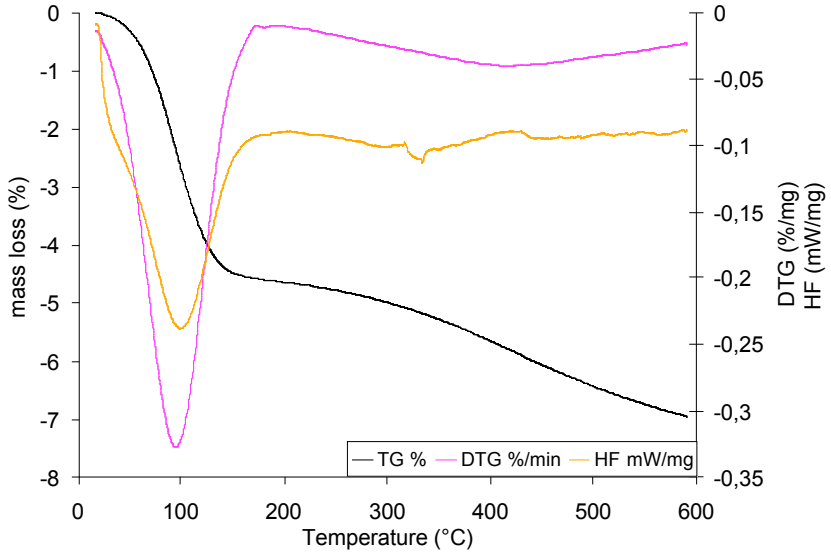

Fig. 3: TG-DSC diagrams for silica gel.

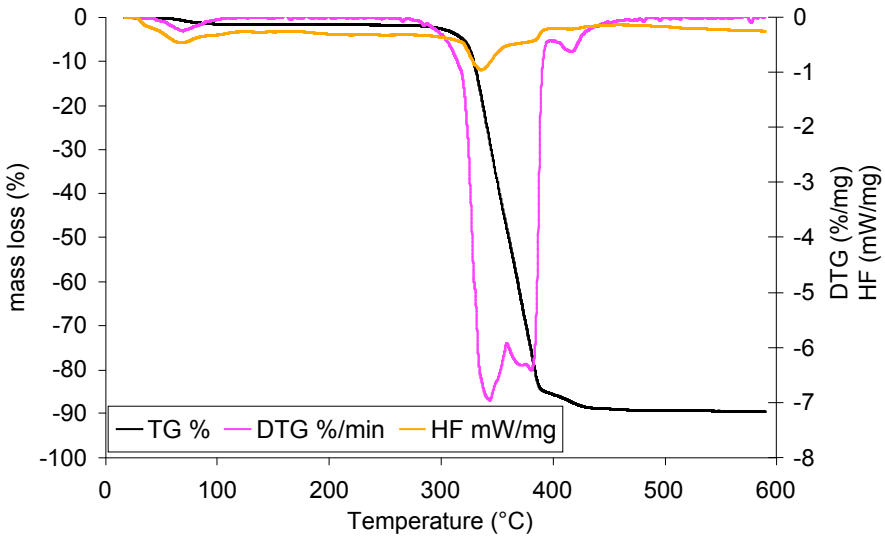

Fig. 4: TG-DSC diagrams for $MgSt_2$.

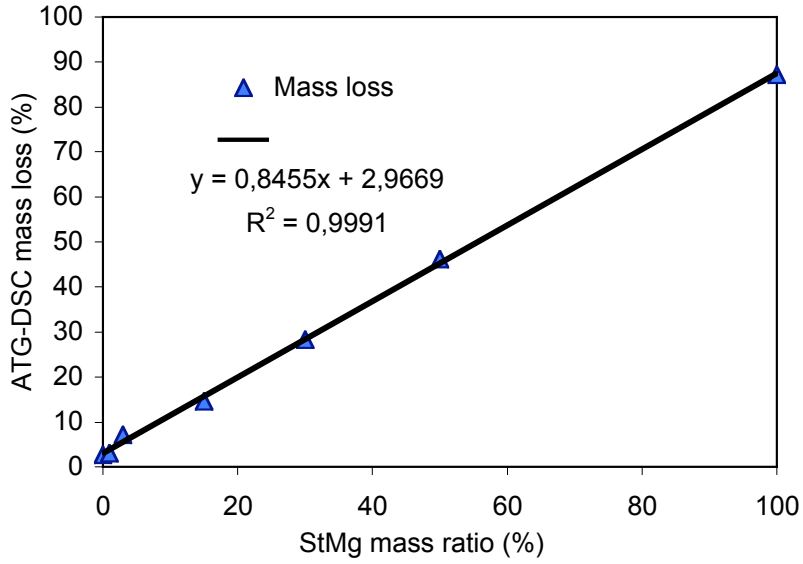

Fig. 5: Experimental relation between the TG-DSC mass loss (from 250°C to 600°C) and the mass ratio of $MgSt_2$.

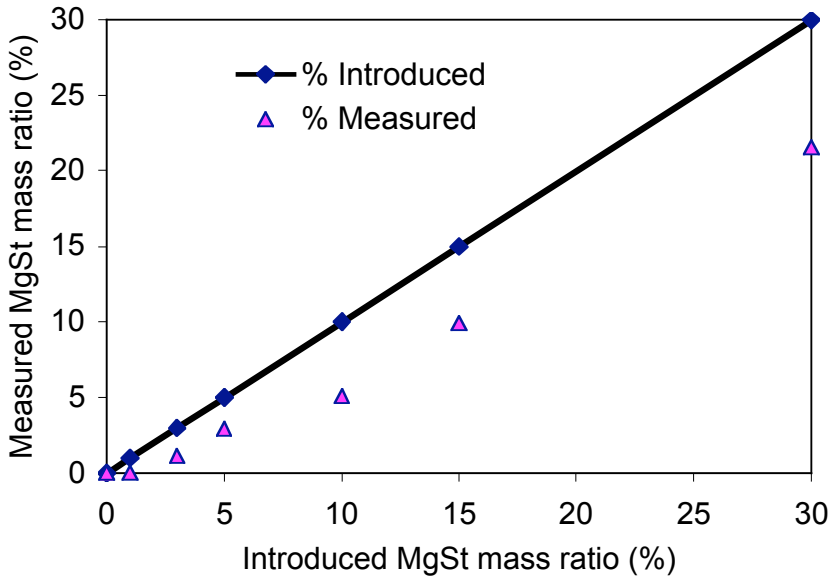

Fig. 6: Real mass fraction of $MgSt_2$ after the coating process calculates from the mass loss.

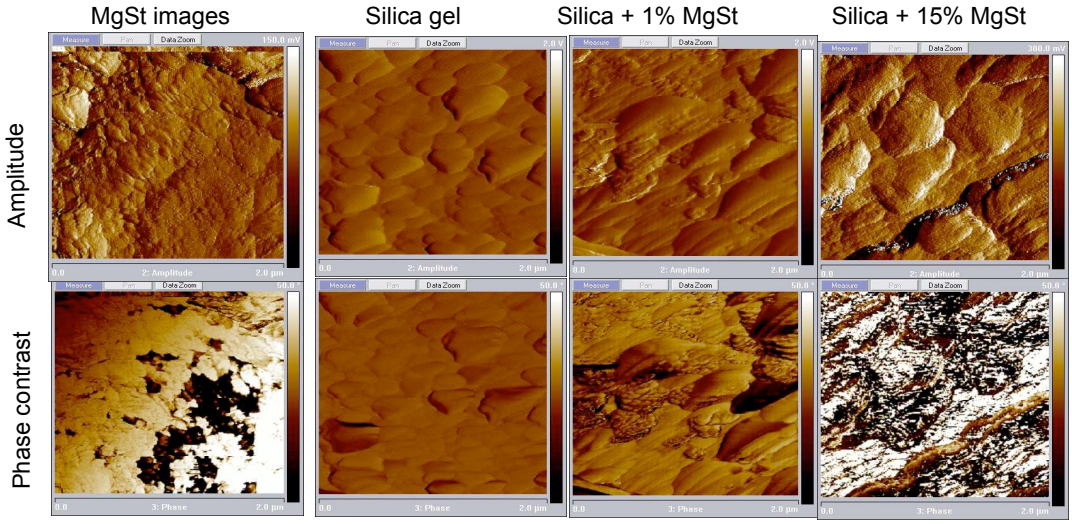

Fig. 7: TM-AFM images of $MgSt_2$, silica gel and silica coated with 1% and 15 % initial mass ratios of $MgSt_2$ (2x2 μm^2).

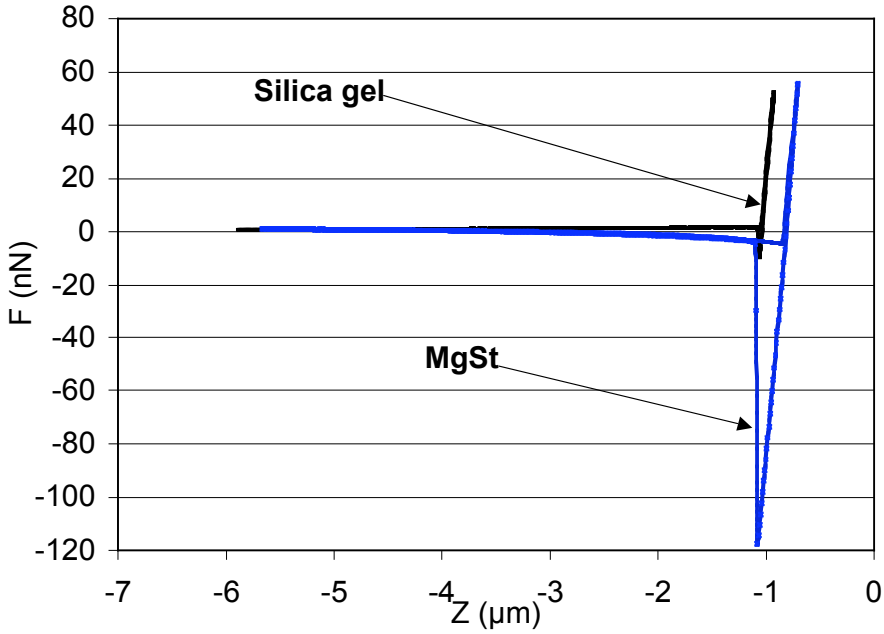

Fig. 8: Force curves F (N/m) as a function of the distance z (µm) measured with $MgSt_2$ sticked on the tip for pure silica gel and pure $MgSt_2$.

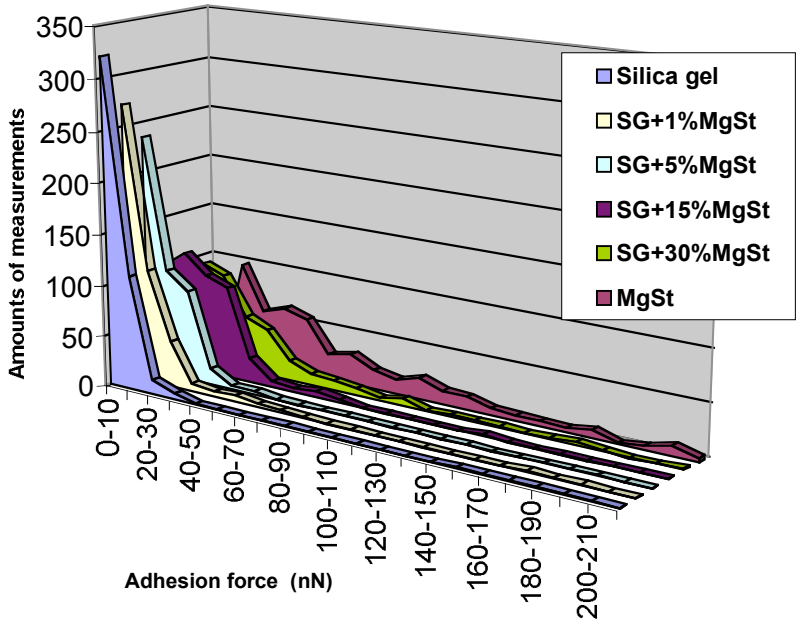

Fig. 9: CM-AFM adhesion force distribution obtained with 450 analyses for different particulate systems.

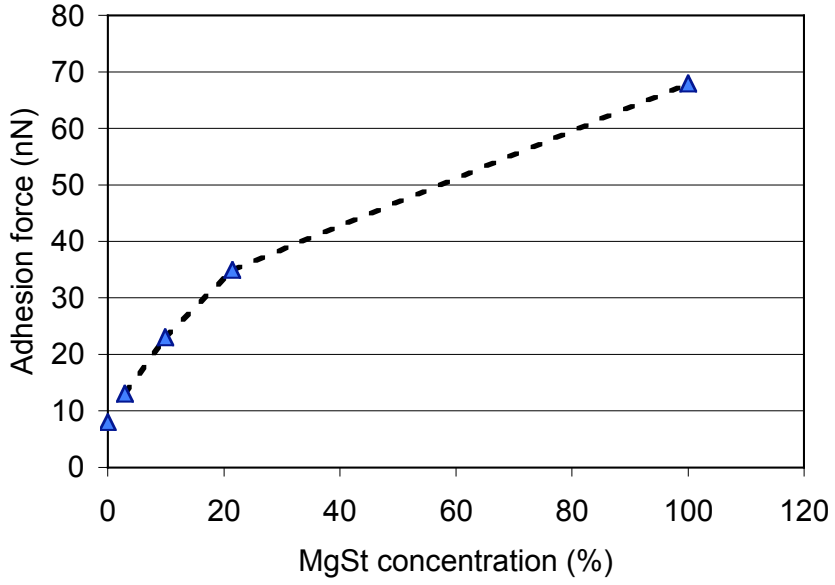

Fig. 10: Mean adhesion force (nN) as a function of the sample $MgSt_2$ concentration.

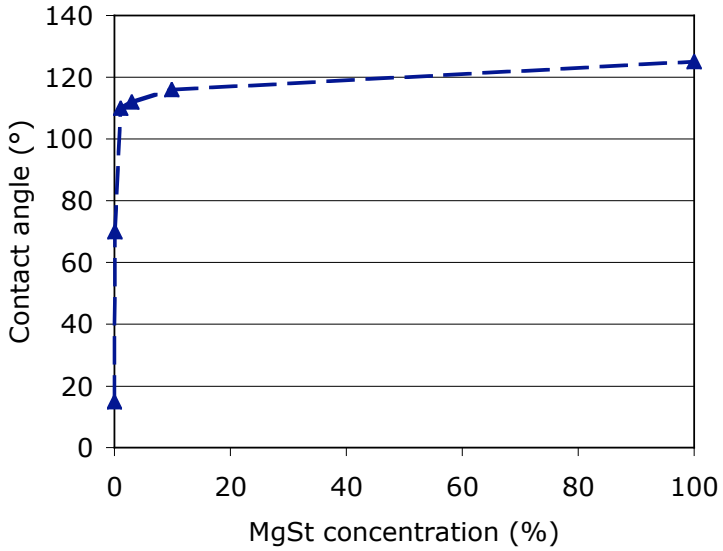

Figure 11: Contact angle measurements (°) as a function of the sample $MgSt_2$ concentration.